



In Silico Molecular Docking Approach of Brassica Oleracea L. Var. Italica-Phytochemicals against CDK4 in Retinoblastoma

Sowmya Hari^{1*}, Anusha Rengarajan², Jothika P.S³, MeenambigaSetti Sudharsan⁴, Ivo Romauld S⁵, Manjunathan J⁶, Vardhana J⁷, Thenmozhi M⁸, Aswathy S⁹

^{1,2,3,4,5} Department of Bio-Engineering, School of Engineering,

Vels Institute of Science Technology and Advanced Studies, Chennai, TamilNadu, India.

^{6,7,8,9} Department of Biotechnology, School of Life Sciences,

Vels Institute of Science Technology and Advanced Studies, Chennai, TamilNadu, India.

Email: ¹sowmya.se.@velsuniv.ac.in

Abstract

Retinoblastoma is a malicious intraocular tumour common in children, accounting for around 4% of all childhood cancers. Light is detected by the retina, a thin layer of nerve cells, which then transforms it into nerve signals that are sent to the brain through the optic nerve. The incidence of the retinoblastoma is due to the biallelic deletion of the RB1 gene as well as other genetic and epigenetic changes that leads to cancer growth. The absence of RB1 causes retinoblastoma cells highly vulnerable to malignant transformation. Chemotherapy has improved treatment outcomes, and novel ways of targeted medication delivery have made it possible to preserve the globe. However, more effective and less toxic molecularly targeted therapies are required. *Brassica oleracea L. var. italica* has acquired recognition as nutraceutical foods due to their high quantities of bioactive components such as glucosinolates, polyphenols, carotenoids, minerals, vitamins. *Brassica oleracea L. var. italica* has antitumor potential against a variety of malignancies. This work identifies the potent inhibitors of CDK4 (3G33) for the treatment of retinoblastoma.

Keywords: Retinoblastoma, RB1 gene, active compounds, *Moringaoleifera*, *Brassica oleracea* L. var. *italica*, *in silico* studies.

1. Introduction

Retinoblastoma is a type of cancer that is identified in the children under the age of three and affects about 1 in every 16,000 live births. The retina is a thin layer of nerve cells that converts light to nerve signals which are sent to the brain through the optic nerve (Kaewkhawet *al.*, 2020). Retinoblastoma is regarded the paradigm of heritable tumors because of the apparent linkages between clinical care and genetic causes. In foetuses, newborns, and young children, retinoblastoma develops when RB1 gene, which typically subdues retinoblastoma, are lost from a growing retinal cell. It can affect one (unilateral) or both (bilateral) eyes, and it's linked to a midline brain tumour in 5% of children with heritable retinoblastoma (H1). Retinoblastoma is most likely caused by a growing cone photoreceptor precursor cell that has lost both alleles of the RB1 tumour suppressor gene and is stuck in the inner nuclear layer of the retina, unable to migrate to the outer retina and function normally

(Soliman *et al.*, 2017). Only retinoma, a benign precursor to retinoblastoma, is caused by loss of both RB1 alleles, and other genes are altered to trigger cancer progression (Naruet *et al.*, 2017). The first incidence of a tumour is the development of a white pupillary reflex known as leukocoria, followed by the misalignment of eyes (strabismus). The eye(s) of some of the children who are afflicted can become red, painful and uncomfortable (Al-Nawaiseh *et al.*, 2014). The majority of cases (60 %) are non-hereditary retinoblastoma, with both RB1 alleles locally altered in the afflicted retina. A RB1 germ line-predisposing variation and later somatic inactivation of the other allele are linked to hereditary retinoblastoma (40 %). Retinoblastoma is a treatable cancer with a good chance of ocular survival if diagnosed early, but it is always fatal if left untreated. If treatment is delayed, tumours progress, obstructing eyesight and posing a danger of metastasis (Shields *et al.*, 2006; Yousef *et al.*, 2017). The protein cyclin dependent kinases (CDKs) regulate cell cycle progression in eukaryotic cells. To regulate cell-cycle checkpoints, CDKs work with proteins called cyclins. To divide and replicate, cells must go through the four phases of the cell cycle: G1, S phase (DNA synthesis), G2, and M phase (mitosis). (Shapiro *et al.*, 2006) CDK4 is a major regulator of the G1–S transition. The retinoblastoma (Rb) protein is phosphorylated by Cyclin D1 (CCND1), which forms a complex with CDK4 and inactivates it. Rb-mediated repression of the transcription factor E2F, which commits the cell to progression through the cell cycle, is relieved as a result. Although the CDK4/cyclin D1 complex is assumed to primarily regulate Rb, current research has revealed the transcription factor FOXM1 as another possible phosphorylation target. However, the therapeutic implications of this transcription factor are still unknown. (Dickson *et al.*, 2014) Ser/Thr kinase in cyclin D-CDK4 (DC) complexes regulate the cell cycle during the G1/S transition and it phosphorylates members of the retinoblastoma (RB) protein family, including RB1. Phosphorylation and inactivation of pRb results in the activation of E2F target genes, which aids cell cycle progression through the G1 phase, eventually leading to retinoblastoma. (Sivashanmugam *et al.*, 2013). Natural substances have an advantage over chemical antagonists in that they are a safer alternative with fewer/no adverse effects. This is an *in silico* study to see whether plant-based therapeutic molecules have the ability to bind to CDK4 and can be used in the treatment of retinoblastoma.

Brassica oleracea L. var. Italica

Brassica oleracea L. var. Italica is a cabbage-like green plant with large flowers that is used as vegetable. (Mirajet *et al.*, 2016). Broccoli seedlings were found having high phytochemicals that promote health, such as nitrogen-sulfur derivatives (glucosinolates and isothiocyanates), minerals (selenium, potassium, and manganese), polyphenols (chlorogenic and sinapic acid derivatives, and flavonoids), and vitamins (A, C, K, and B6). (Le TNet *et al.*, 2020) According to existing research, eating broccoli sprouts and microgreens as part of a dietary serving improves human health and lowers the risk of chronic diseases. In recent years, the anti-cancer and anti-oxidant effects in particular have been extensively researched. Furthermore, human studies have shown that broccoli seedlings have the ability to act as a preventive agent against a variety of cancers and other disorders. (Ravikumaret *et al.*, 2015)

2. Materials and Methods

Macromolecule selection and preparation

The target protein cyclin dependent kinase-4 (PDB ID- 3G33), retrieved from Protein Data Bank (PDB) (<http://www.rcsb.org>). PDB is the global repository of empirically confirmed three dimensional structures of proteins and their complexes. A four-character PDB identification is assigned to each archival record. The PDB archive offers detailed descriptions of crystallographic, NMR, and 3DEM structural models. (Burley SKet al.,2017)The protein (Id 3G33) was found to be a heterotetramer with similar A and C chain, B and D chains respectively. Only chain A and B were docked. The protein was prepared by removing the water molecules and adding Kollman and Gasteiger charges using Autodock tools from MGL Tools package <http://mgltools.scripps.edu/>. (Sastry et al.,2013)

Active compounds identification

Active compounds in *Brassica oleracea* were identified from literatures. Sixteen compounds namely: Butyl isothiocyanate, Gluconapin, Glucocochlearin, Glucoiberberin, Glucosativin, Glucoerucin, Gluconasturtiin, Butyronitrile, Allylisothiocyanate, 2-methyl-2-nitropropane, Iberin, Indole-3-carbinol, Indole-3-carboxylic acid, indole-3-acetic acid and Isorhamnetin was selected based on their medicinal properties and was used in the docking studies. The molecular docking study was carried out against the control drug Carboplatin, prescribed for the retinoblastoma patients. The structure of ligand and the Carboplatin was taken from the Pubchem (<https://pubchem.ncbi.nlm.nih.gov>). The structure of active compounds in SDF format was taken from PubChem and the structure was changed to PDB format using PyMOL software. Substance, Compound, and BioAssay are the three databases that PubChem organises its data into. Depositor-contributed descriptions of chemical substances are included in the Substance database. The Compound database stores chemical structures that have been retrieved from the Substance database via structural standardisation. The BioAssay database offers information about biological assay experiments as well as their outcomes. (Kim Set al.,2019)

PyMOL, a cross-platform molecular graphics programme, used to visualise proteins, tiny molecules, nucleic acids, surfaces, electron densities, and trajectories in three dimensions. PyMOL is currently one of the most extensively used macromolecular visualisation programmes. (Yuan Set al.,2017). The structure and the therapeutic applications of the ligands are given in Table 1

Prediction of drug-likeness property in the active compounds

The Drug like ability of all the active compounds was tested using Molinspiration server. (<https://www.molinspiration.com>). Drug-likeness property is a concept that helps with pharmacokinetic and pharmacological properties like solubility, chemical stability, bioavailability, and distribution profile optimization. (Ursu et al.,2011). Bioavailability issues may arise if molecules fail to meet more than one of these requirements. (<https://www.molinspiration.com/services/properties.html>)

CASTp for Active site prediction

The active site of the target protein was predicted using CASTp server (<http://sts.bioe.uic.edu/castp>) and the pocket regions of the protein, Cyclin dependent kinase-

4 (PDB ID- 3G33) was identified. The CASTp web service intends to give a thorough and detailed quantitative analysis of protein's surface pockets and interior voids, which are significant concave regions typically involved with binding processes. CASTp locates all pockets and voids in a protein structure and delineates the atoms involved in their production in detail. **(Binkowski *et al.*,2003)**

Molecular Docking and Visualization

The major tool employed in computer assisted drug design is Molecular docking. Molecular docking programmes use a search technique that determines the conformation of the ligand repeatedly until it converges to the minimal energy. Finally, the sum of the electrostatic and van der Waals energies is used to rank the candidate postures using an affinity scoring function, $G [U \text{ total in kcal/mol}]$. **(NSet *et al.*,2017)** The computational tool, Autodock 4.2 is used for the docking of the ligands to the proteins. AutoDock uses a Lamarckian genetic algorithm to predict ligand conformation **(Rizviet *et al.*,2013)**. The ligand-protein interaction with the least negative ΔG implies a strong binding and desirable conformation. **(Africa *et al.*,2018)**. The graphical user interface, Discovery studio Visualizer, was used to see docked structures in 2D and 3D. Accelrys Discovery Studio Visualizer is a free programme for visualising macromolecule-ligand interactions. Small molecules and large macromolecules are studied using this software. **(Jejurikar *et al.*,2021)**

3. Result and Discussion

Retinoblastoma is the most prevalent type of paediatric eye cancer and is fatal it is not treated. According to predictions, the majority of retinoblastoma incidences occur in Asia (53 percent), followed by Africa (29 percent), Latin America (8 percent), North America (3 percent), and Europe (3 percent) (6 percent). Globally retinoblastoma survival rate is around 30% **(Ancona-Lezama *et al.*,2020)** Every year, roughly 1500 new cases are reported in India, accounting for 33% of the global burden and a mortality rate of up to 24%. **(Beniwal *et al.*,2022)**. The statistics show a dire need for the timely detection, treatment of retinoblastoma with minimal side effects and optimization of the vision in the low-and-middle-income countries (LMICs).

Cycle-independent kinases 4 and 6 (CDK4 and CDK6) and their activation partner, type D cyclins, connect the outside environment to the inner cell cycle mechanism. Continuous activation of cyclin D-CDK4 / 6 is the driving force behind tumorigenesis in several types of cancer. New CDK4/6 inhibitors have been identified and are now being studied in preclinical and clinical studies for the treatment of several cancer types. **(Fassl *et al.*,2022)**

16 plant phytochemicals with therapeutic ability were chosen to inhibit CDK4 (PDB ID- 3G33) in this study. Pubchem was used to determine the structure of these ligands (Table 1). CDK4's structure was acquired from the Protein Data Bank (PDB). PyMol was used to eliminate any excess chains and water molecules from the proteins, and the final protein file was saved as a PDB file (Figure 1). The pharmacological potential of all the ligands was assessed using Lipinski's rule of five for in silico study of plant compounds. The molecular properties of the ligands in the Lipinski's rule were studied using the Molinspiration website. The molecular weight, number of hydrogen donors, acceptors, and lipophilicity of the ligand molecules are among the results. Out of the 20 compounds studied, 16 compounds cleared

Lipinski's rule of five. Progoitrin, Glucoiberin, Neoglucobrassicin, Tannic acid showed violations; hence, the compound was eliminated from further docking analysis. Table 2 shows the Lipinski characteristics of plant *Brassica oleracea* L. var. *Italica*. Active site pockets in CDK4 (PDB ID- 3G33) was determined using CASTp (Figure 2). CASTp is a web-based tool to determine the amino acid residues in the active pocket of the proteins. CASTp results are depicted in Figure 3 for 3G33(chain A) and Figure 4 for 3G33(chain B). CASTp was used to find active site pockets in CDK4 (PDB ID 3G33) (Figure 2). CASTp (Computed Atlas of Surface Topography of Proteins) is an online tool to determine the catalytic amino acids in proteins (Tian *et al.*, 2018). Figure 3 shows the CASTp results for 3G33(chain A) and Figure 4 shows the CASTp results for CDK4 (chain B). The active site amino acids and their locations based on CASTp results are shown in Table 3 for CDK4 (chain A and chain B). All 16 compounds were docked and their binding potential with CDK4 Chain A and Chain B was analysed using Autodock 4.2. AutoDock, a computational tool was created to give a method for predicting small molecule interactions with macromolecular targets that can quickly distinguish between compounds with micromolar and nanomolar binding constants and can frequently rank compounds with smaller affinity differences. (Rizvi *et al.*, 2013) Tables 4 and 5 show the binding energy, number of hydrogen bond interactions, and amino acids involved in the interactions for CDK4(chain A) and CDK4(chain B) respectively.

Isorhamnetin, a monomethoxyflavonol ligand, has the lowest binding energy of -6.59 kcal/mol among the molecules docked with CDK4, Chain A. ALA167, SER171, TYR22, THR177, ALA175, LEU176, and TYR170 are the seven hydrogen bonds formed. (Fig. 5) The expression of AKT2 mRNA, miR-1, and miR-3163 are up-regulated by the Isorhamnetin. (Matboli *et al.*, 2021) The miR-3163 plays a variety of roles in various types of illness and malignancies. In retinoblastoma cancer stem cells, it can alter proliferation, apoptosis, and drug resistance. (Jia *et al.*, 2016) Indole-3-acetic acid, an isothiocyanate (ITCs) had a good binding energy of -6.29 kcal/mol and had a hydrogen bond interaction with the ALA21, THR177, and LEU176 (Fig. 6). ITC induces Kelch-like ECH-associated protein 1 (Keap1) and nuclear factor erythroid 2-related factor 2 (Nrf2) in the ARE (antioxidant response elements) pathway, which protects normal cells from oxidative stress by stimulating chemoprotective genes (NQO1) (Bao *et al.*, 2014) Indole-3-carbinol and Indole-3-carboxylic acid resulted in the binding energy of -6.00 kcal/mol and -6.13 kcal/mol having H-bond interaction with, LEU277, LEU234, ARG260 and ARG10, TYR11, THR95 (Fig. 7) respectively. All the other compounds including, Butyl isothiocyanate, Gluconapin, Glucocochlearin, Glucoiberin, Glucosativin, Glucoerucin, Gluconasturtiin, Butyronitrile, Allyl isothiocyanate, 2-Methyl-2-nitropropane and Iberin had their binding energies lower than Carboplatin, which showed -5.38 kcal/mol.

Whilst in the chain B of CDK4, Indole-3-acetic acid had least binding energy of -6.69 kcal/mol, forming hydrogen bond contacts with ARG95, CYS47, and ARG50 (Fig. 8). The compound Indole-3-carboxylic acid had a binding energy of -6.37 kcal/mol (Fig. 9). Glucoiberin a Glucosinolates (GLS) showed a binding energy of -6.04 kcal/mol respectively. Indole-3-carbinol and Isorhamnetin gave a binding energy of -5.99 kcal/mol and -5.49 kcal/mol. (Fig. 10) The Glucocochlearin and 2-Methyl-2-nitropropane had binding

energy of -4.27 kcal/mol and -4.61 kcal/mol. The binding energies of all the other compounds were lower than that of the conventional drug Carboplatin, which measured -4.10 kcal/mol.

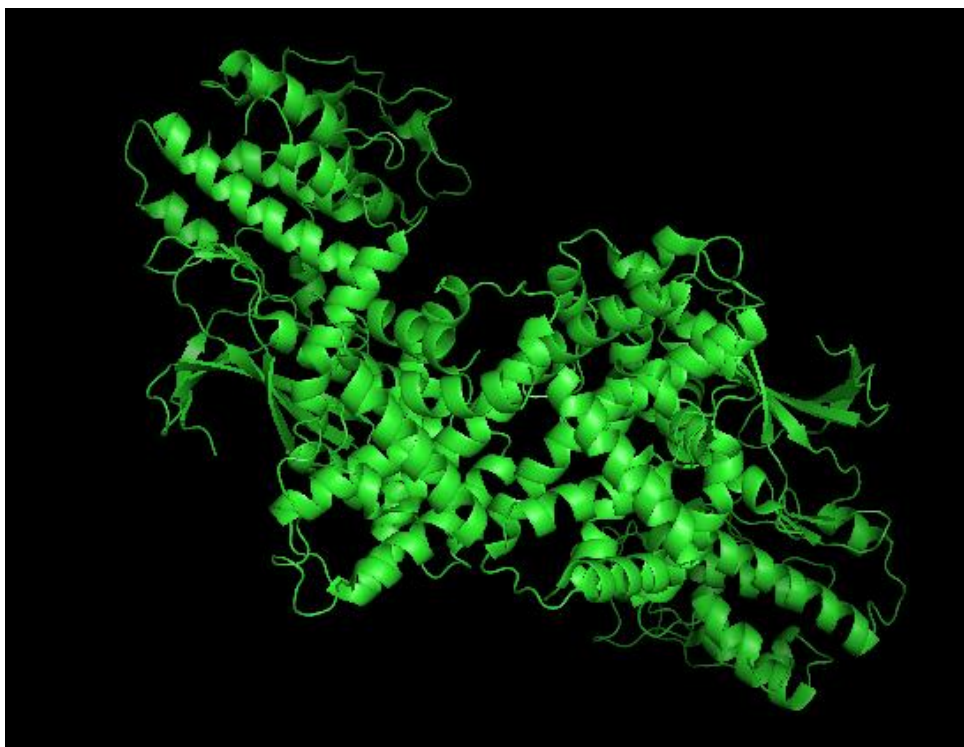


Figure 1. Structure of Cyclin Dependent Kinase

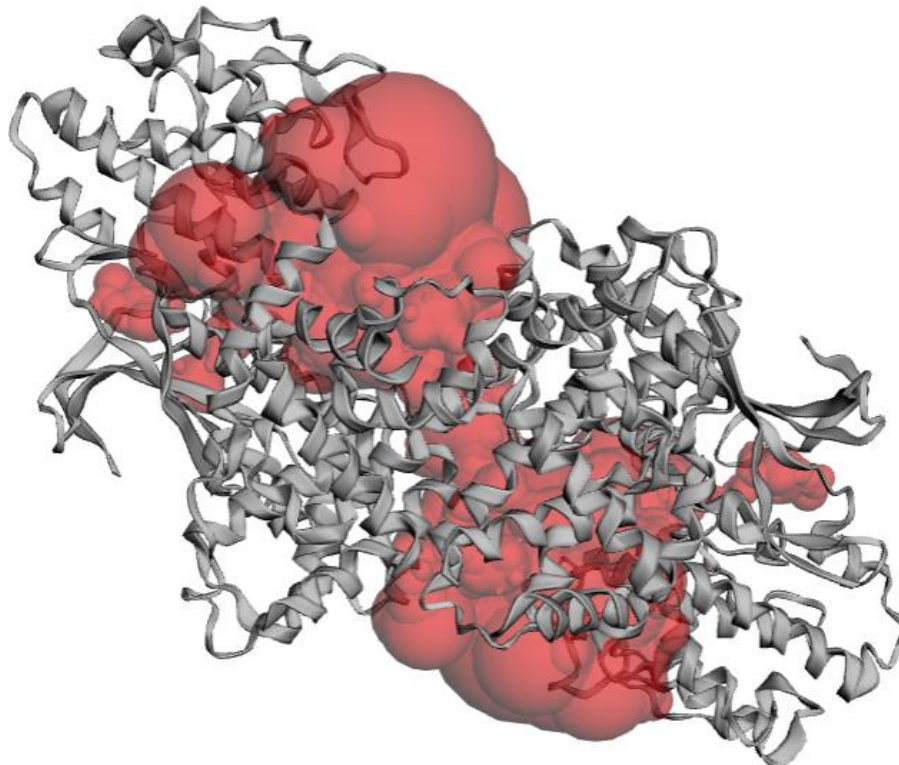
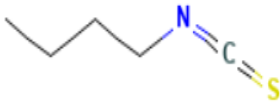
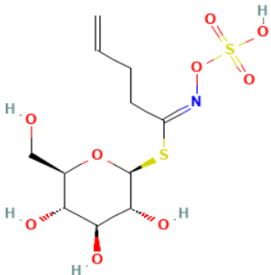
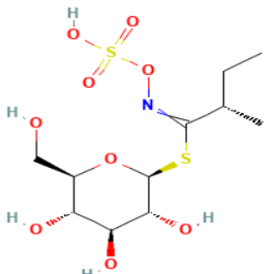
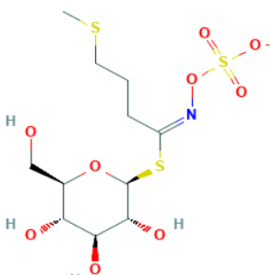
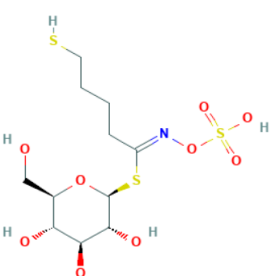
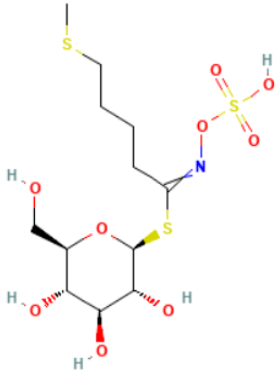
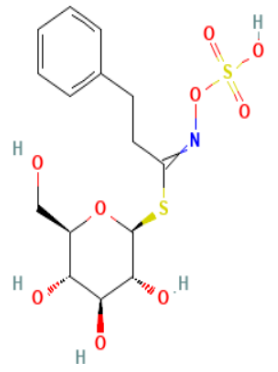
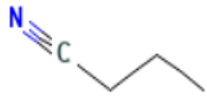
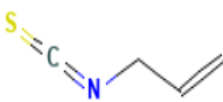
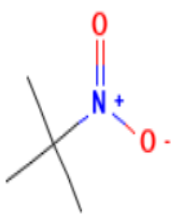


Figure 2. Active site analysis of amino acids of CDK-4 protein using CASTp

Table 1. The structure and the therapeutic applications of the ligands

S.no	Compound	Molecular Formula	Structure	Properties	References
1	Butyl isothiocyanate	C ₅ H ₉ NS		Anti-tumoral, Anti-inflammatory, Neuroprotective, prevents oxidative stress and protection of skin.	(Bao <i>et al.</i> , 2014)
2	Gluconapin	C ₁₁ H ₁₉ NO ₉ S ₂		Anti-microbial, Antioxidant, Cytotoxicity, Anti-cancer.	(Maina <i>et al.</i> , 2020)
3	Glucocochlearin	C ₁₁ H ₂₁ NO ₉ S ₂		Anti-carcinogenic and Anti-microbials	(Deng <i>et al.</i> , 2015)
4	Glucoiberberin	C ₁₁ H ₂₀ NO ₉ S ₃		Tumor growth inhibition, Anti-microbial	(Al-Gendy <i>et al.</i> , 2016)
5	Glucosativin	C ₁₁ H ₂₁ NO ₉ S ₃		Cytoprotective, Anti-cancer, Anti-ulcer, diuretic, hepatoprotective.	(Jaafar <i>et al.</i> , 2019)

6	Glucoerucin	C ₁₂ H ₂₃ NO ₉ S ₃		Anti-microbial, Bone Formation, Cholinesterase Inhibitory Activity.	(Baoet <i>et al.</i> ,2014)
7	Gluconasturtiin	C ₁₅ H ₂₁ NO ₉ S ₂		Anti-fungal, Anti-microbial, Anti-bacterial.	(Choi <i>et al.</i> ,2017)
8	Butyronitrile	C ₄ H ₇ N		Free radical scavenging and Anti-oxidant	(Chaudhary <i>et al.</i> ,2014)
9	Allylthiocyanate	C ₄ H ₅ NS		Anti-angiogenic, Anti-cancer activities.	(Liu <i>et al.</i> ,2018)
10	2-Methyl-2-nitropropane	C ₄ H ₉ NO ₂		Anti-oxidant and Anti-proliferative activities.	(Chaudhary <i>et al.</i> ,2014)

11	Iberin	C ₅ H ₉ NOS ₂		Inhibition of cell proliferation, Anti-metastasis and Anti-angiogenesis.	(Pocasapet <i>et al.</i> , 2019)
12	Indole-3-carbinol	C ₉ H ₉ NO		Anti-proliferative and Anti-carcinogenic	(Fujioka <i>et al.</i> , 2016)
13	Indole-3-carboxylic acid	C ₉ H ₇ NO ₂		Activators of human adenosine monophosphate-activated protein kinase (AMPK) and Acetylcholinesterase inhibition activity.	(Ryder <i>et al.</i> , 2018 and Melonget <i>et al.</i> , 2018)
14	Indole-3-acetic acid	C ₁₀ H ₉ NO ₂		Anti-bacterial, Anti-fungal, Anti-oxidant, Anti-cancer and wound healing.	(Chitra <i>et al.</i> , 2017)
15	Isorhamnetin	C ₁₆ H ₁₂ O ₇		Anti-inflammatory, Anti-tumour, Anti-oxidation, cardiovascular and cerebrovascular protection	(Gong <i>et al.</i> , 2020)

Table 2: The Lipinski characteristics of plant *Brassica oleracea* L. var. *Italica*.

S. No	Compound	LogP	Molecular weight	Hydrogen-bond donor	Hydrogen-bond acceptor	No. of violations
1	Carboplatin	-0.45	144.13	2	4	0
2	Butyl isothiocyanate	3.04	115.2	0	1	0
3	Progoitrin	-4.24	389.4	6	11	2
4	Gluconapin	-3.12	373.4	5	10	0
5	Glucocochlearin	-2.92	375.42	5	10	0
6	Glucoiberin	-4.43	406.48	4	10	0
7	Glucosativin	-3.18	407.49	5	10	0
8	Glucoiberin	-4.7	423.49	5	11	1
9	Glucoerucin	-2.97	421.51	5	10	0
10	Gluconasturtiin	-2.22	423.46	5	10	0
11	Butyronitrile	0.94	69.11	0	1	0
12	Allylisothiocyanate	2.25	99.16	0	1	0
13	2-methyl-2-nitropropane	1.28	103.12	0	3	0
14	Iberin	0.88	163.27	0	2	0
15	Indole-3-carbinol	1.43	147.18	2	2	0
16	Indole-3-carboxylic acid	1.66	161.16	2	3	0
17	Indole-3-acetic acid	1.51	175.19	2	3	0
18	Isorhamnetin	1.99	316.26	4	7	0
19	Neoglucobrassicin	-2.56	478.5	5	12	1
20	Tannic acid	7.06	1701.2	25	46	4

Chain A



Figure 3. The amino acids involved in formation of catalytic site of CDK4 (PDB ID- 3G33), chain A. Active site residues are indicated by letters that are highlighted in blue.

Chain B



Figure 4. The amino acids involved in formation of catalytic site of CDK4 (PDB ID- 3G33), chain B. Active site residues are indicated by letters that are highlighted in blue.

Table 3. CASTp provided a list of active site amino acids found in CDK4.

Amino acid	Position	Amino acid	Position
Isoleucine	17	Glycine	23
Valine	19	Aspartic acid	24
Tyrosine	22	Arginine	26
Glycine	23	Serine	30
Serine	41	Leucine	31
Leucine	65	Tryptophan	63
Glutamic acid	72	Valine	67
Histidine	73	Glutamine	71
Arginine	106	Cysteine	73
Aspartic acid	134	Glutamic acid	74
Asparagine	139	Threonine	116
Lysine	147	Proline	118
Phenylalanine	164	Lysine	123
Glutamine	173	Isoleucine	126
Methionine	174	Tyrosine	127
Alanine	175	Histidine	158
Threonine	177	Alanine	162
Proline	178	Phenylalanine	163
Tryptophan	243		

Table 4. Docking analysis of plant compounds with 3G33, Chain A

S. no	Compound	Binding Affinity kcal/mol	Number of H ₂ Bonds	H ₂ bonds interaction residues	Other interaction residues	Number of polar and non-polar interactions
1	Carboplatin	-5.38	3	CYS83, ARG10, TYR11	-	3
2	Butyl isothiocyanate	-4.19	3	GLU72, LEU68, HIS73	LEU65, PHE164, LEU79	6

S. no	Compound	Binding Affinity kcal/mol	Number of H ₂ Bonds	H ₂ bonds interaction residues	Other interaction residues	Number of polar and non-polar interactions
3	Gluconapin	-3.88	4	ALA175, GLY23, LEU176, THR177	MET174, TYR170, PRO178, TYR22	8
4	Glucocochlearin	-3.57	2	LYS230, LEU218	LYS216, CYS220	4
5	Glucosiberverin	-4.07	2	ARG260, VAL265	ARG214, LYS216	4
6	Glucosativin	-2.56	3	SER171, ALA21, LEU176	GLN173, TYR170	5
7	Glucosericin	-3.44	5	ARG106, VAL19, THR117, LYS147, THR182	LEU183, TRP184, VAL180	8
8	Gluconasturtin	-4.06	1	LEU176	ALA175, TYR170, MET174, PRO178, ALA21	6
9	Butyronitrile	-4.02	1	HIS73	PHE164, LEU68, VAL76	4
10	Allylisothiocyanate	-4.23	-	-	LEU68, ARG78, VAL76, PHE98	4
11	2-Methyl-2-nitropropane	-4.97	1	ARG10	TYR11, CYS83, LEU39	6
12	Iberin	-4.44	4	ALA175, LEU176, THR177, TYR22	TYR170, PRO178	6
13	Indole-3-carbinol	-6	3	LEU277, LEU234, ARG260	ILE235, VAL262, LEU278, VAL265	7
14	Indole-3-carboxylic acid	-6.13	3	ARG10, TYR11, THR95	LEU39, PRO13, CYS83	6
15	Indole-3-acetic acid	-6.29	3	ALA21, THR177, LEU176	TYR170, ALA175	5
16	Isorhamnetin	-6.59	7	ALA167, SER171, TYR22, THR177, ALA175, LEU176, TYR170	PRO178	8

Table 5. Docking analysis of plant compounds with 3G33, Chain B

S. no	Compound	Binding Affinity kcal/mol	No of H Bonds	H bonds interaction residues	Other interaction residues	No. of direct contacts (polar and non-polar interactions)
1	Carboplatin	-4.10	3	ARG50, PRO93, ARG95	-	3
2	Butyl isothiocyanate	-3.94	1	HIS158	GLU69, GLU75, CYS68	4

S. no	Compound	Binding Affinity kcal/mol	No of H Bonds	H bonds interaction residues	Other interaction residues	No. of direct contacts (polar and non-polar interactions)
3	Gluconapin	-3.60	4	ARG87,ARG41,ARG37,LYS149	LEU148	5
4	Glucocochlearin	-4.27	2	ARG87,ASP151	ARG41	3
5	Glucoiberverin	-6.04	5	LYS147,ARG87,CYS91,SER90,ARG41	LYS149	6
6	Glucosativin	-3.43	3	ALA162,HIS158,GLU74	GLU76	4
7	Glucoerucin	-2.98	2	ARG37, LYS147	LYS149	3
8	Gluconasturtiin	-4.05	3	LYS53,GLN49,ILE52	HIS55,PRO54	5
9	Butyronitrile	-3.72	1	PHE78	LEU65	2
10	Allylisothiocyanate	-3.86	-	-	GLU75,GLU69,CYS73,PHE78	4
11	2-Methyl-2-nitropropane	-4.61	3	ARG26,ASP24,GLN25	-	3
12	Iberin	-4.99	1	ARG57	ASP86	2
13	Indole-3-carbinol	-5.99	4	ARG57,CYS189,ASP192,PRO79	ILE203,ALA190,ALA157	7
14	Indole-3-carboxylic acid	-6.37	4	ARG50,PRO93,ARG95,CYS47	VAL48	5
15	Indole-3-acetic acid	-6.69	3	ARG95,CYS47,ARG50	VAL48,PRO93	5
16	Isorhamnetin	-5.49	3	ARG41,PRO40,MET197	PRO199,VAL39,ARG37	6

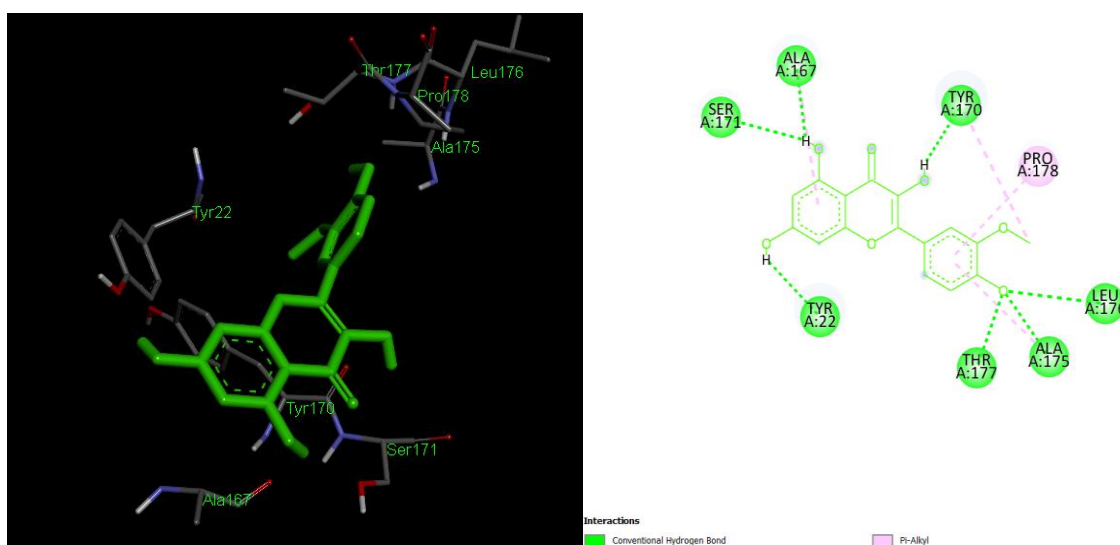


Figure 5. Binding analysis of Isorhamnetin with CDK-4(3G33), chain A and its interactions - 2D and 3D

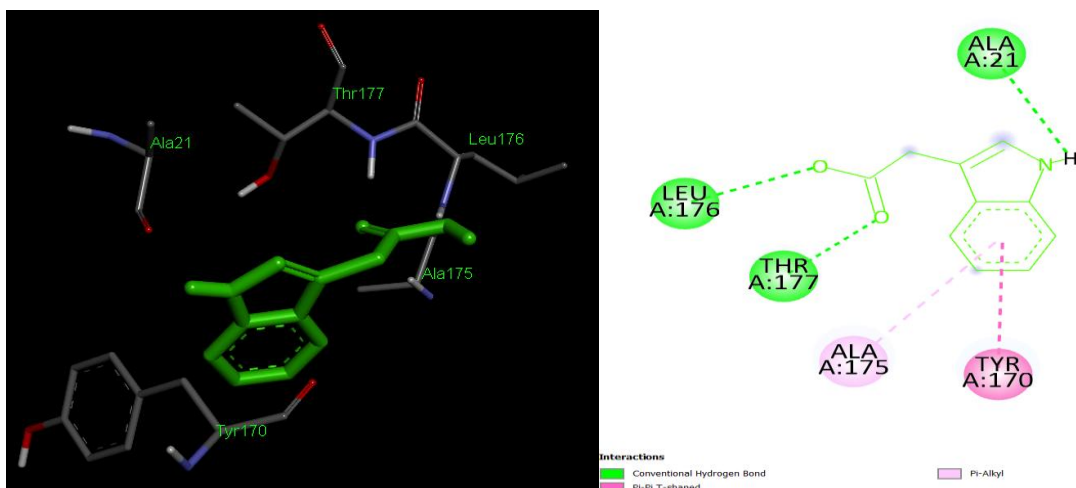


Figure 6. Binding analysis of Indole-3-acetic acid with CDK-4(3G33), chain A and its interactions -2D and 3D

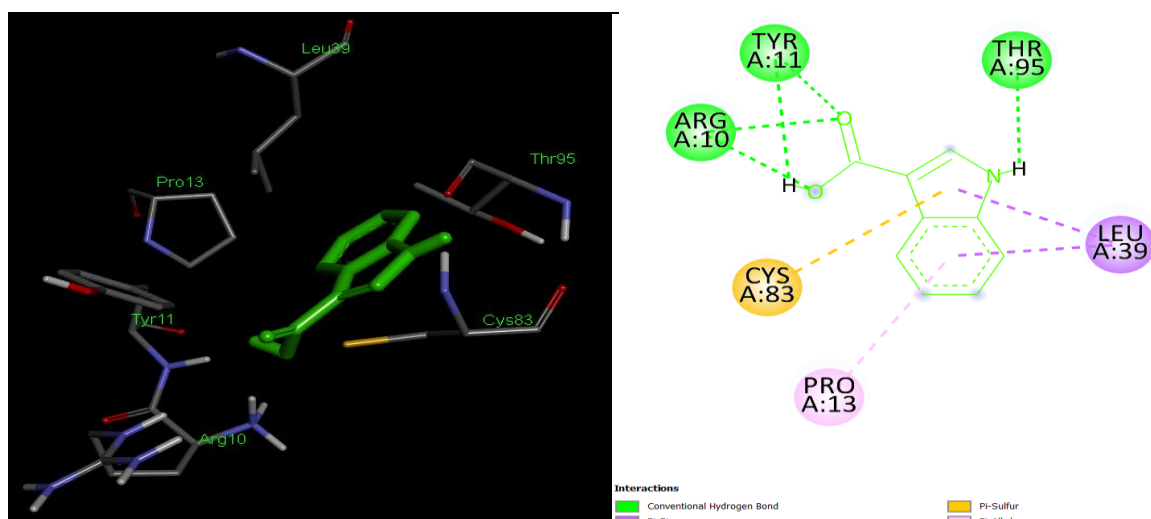


Figure 7. Binding analysis of Indole-3-carboxylic acid with CDK-4(3G33), chain A and its interactions -2D and 3D

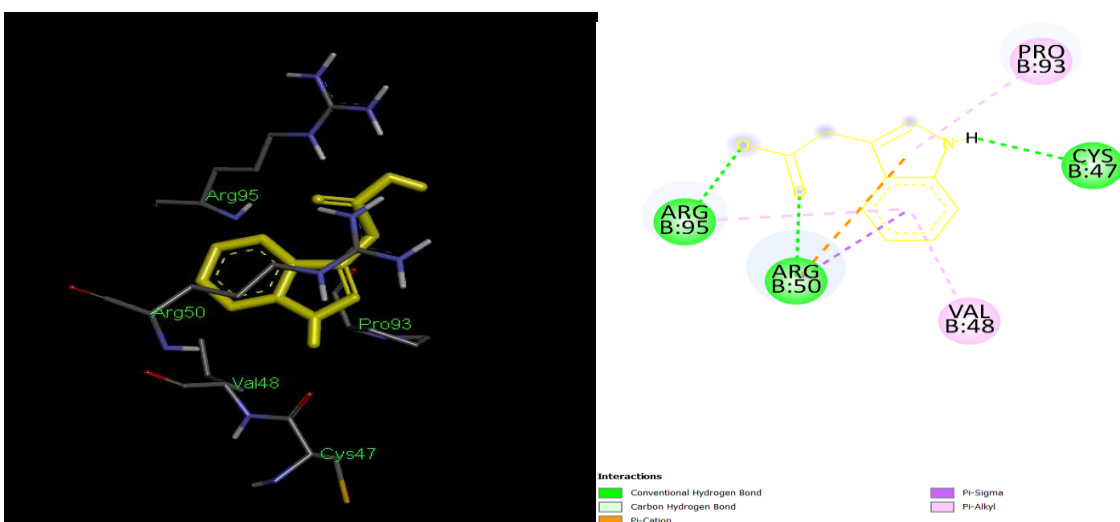


Figure 8. Binding analysis of Indole-3-acetic acid with CDK-4(3G33), chain B and its interactions -2D and 3D

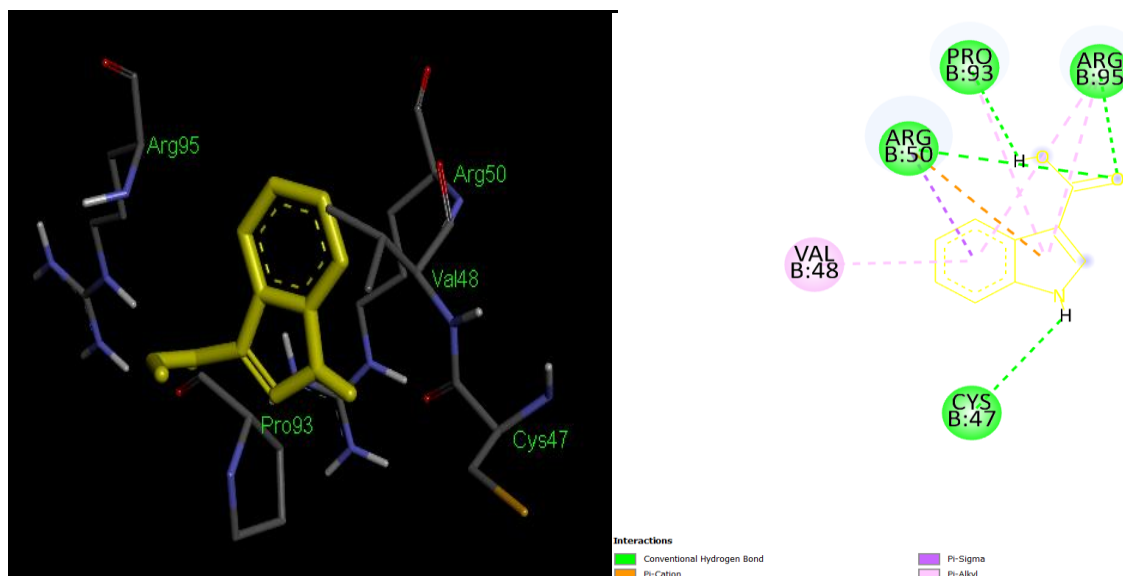


Figure 9. Binding analysis of Indole-3-carboxylic acid with CDK-4(3G33), chain B and its interactions -2D and 3D

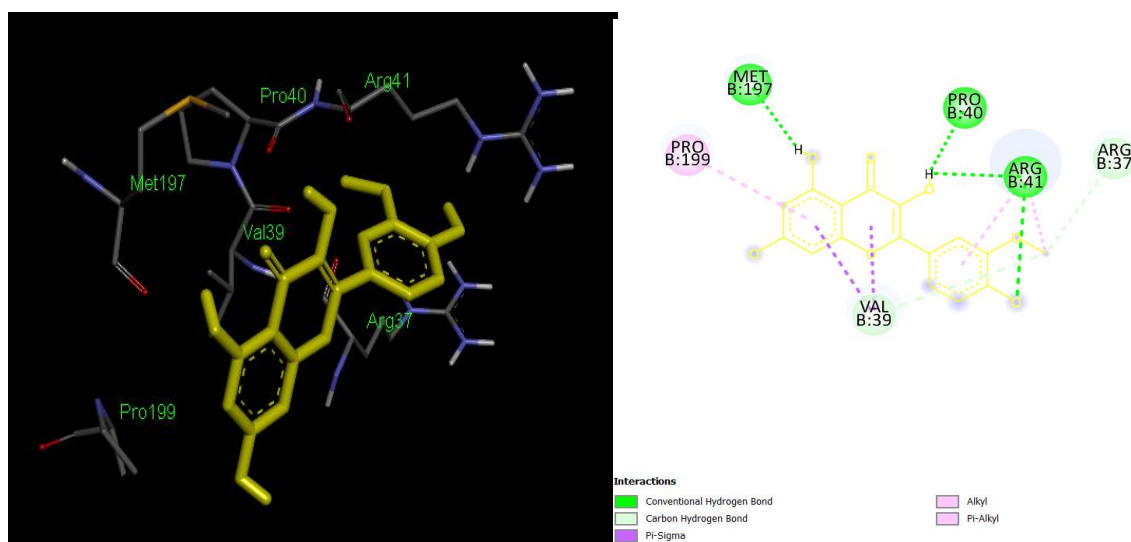


Figure 10. Binding analysis of Isorhamnetin with CDK-4(3G33), chain B and its interactions -2D and 3D

4. Conclusion

The medications that are used to treat retinoblastoma have a variety of negative effects. As a result, finding novel drugs that target and treat retinoblastoma with minimal side effects is essential. Therapeutically active molecules from plant, *Brassica oleraceaL.var.Italica* were investigated using Molecular Docking against CDK4. The phytochemicals namely, Isorhamnetin, Indole-3-acetic acid and Indole-3-carboxylic acid had a good binding affinity in both the chains A, B of the protein CDK4. As a result, further *in-vitro* investigations can be conducted on these compounds, for the development of a possible medication for the treatment of retinoblastoma tumours.

Conflicts of interest

Authors declare that there are no Conflicts of interest

References

- [1] Kaewkhaw R, Rojanaporn D. Retinoblastoma: etiology, modeling, and treatment. *Cancers*. 2020 Aug;12(8):2304.
- [2] Soliman SE, Racher H, Zhang C, MacDonald H, Gallie BL. Genetics and molecular diagnostics in retinoblastoma—an update. *The Asia-Pacific Journal of Ophthalmology*. 2017 Mar 1; 6(2):197-207.
- [3] Naru J, Aggarwal R, Mohanty AK, Singh U, Bansal D, Kakkar N, Agnihotri N. Identification of differentially expressed proteins in retinoblastoma tumors using mass spectrometry-based comparative proteomic approach. *Journal of proteomics*. 2017 Apr 21; 159:77-91.
- [4] Al-Nawaiseh I, Jammal HM, Khader YS, Jaradat I, Barham R. Retinoblastoma in Jordan, 2003-2013: ocular survival and associated factors. *Ophthalmic Epidemiol*. 2014;21(6):406–11.
- [5] Shields CL, Shields JA. Basic understanding of current classification and management of retinoblastoma. *Curr Opin Ophthalmol*. 2006;17(3):228–34.
- [6] Yousef YA, Nazzal RM, Khalil MB, Deebajah R, Mehyar M, Hajja S, Mohammad M, Al Jabary R, Jaradat I, Sultan I, et al. Management outcome(s) in eyes with retinoblastoma previously inadequately treated with systemic chemotherapy alone without focal therapy. *Oman J Ophthalmol*. 2017;10(2):70–5.
- [7] Shapiro GI. Cyclin-dependent kinase pathways as targets for cancer treatment. *Journal of clinical oncology*. 2006 Apr 10;24(11):1770-83.
- [8] Dickson, M. A. (2014). Molecular pathways: CDK4 inhibitors for cancer therapy. *Clinical cancer research*, 20(13), 3379-3383.
- [9] Sivashanmugam M, Raghunath C, Vetrivel U. Virtual screening studies reveal linarin as a potential natural inhibitor targeting CDK4 in retinoblastoma. *Journal of pharmacology & pharmacotherapeutics*. 2013 Oct;4(4):256.
- [10] Miraj S. Broccoli (*Brassica oleracea* var. *Italica*): Potential candidate in the health management. *Der Pharmacia Lettre*. 2016;8(14):61-5.
- [11] Le TN, Chiu CH, Hsieh PC. Bioactive compounds and bioactivities of *brassica oleracea* l. var. *italica* sprouts and microgreens: An updated overview from a nutraceutical perspective. *Plants*. 2020 Aug;9(8):946.
- [12] Ravikumar, C. (2015). Therapeutic potential of *Brassica oleracea* (broccoli)—A review. *Int J Drug Dev Res*, 7, 009-010.
- [13] Burley SK, Berman HM, Kleywegt GJ, Markley JL, Nakamura H, Velankar S. Protein Data Bank (PDB): the single global macromolecular structure archive. *Protein Crystallography*. 2017:627-41
- [14] Sastry GM, Adzhigirey M, Day T, Annabhimoju R, Sherman W. Protein and ligand preparation: parameters, protocols, and influence on virtual screening enrichments. *Journal of computer-aided molecular design*. 2013 Mar; 27(3):221-34.
- [15] Kim S, Chen J, Cheng T, Gindulyte A, He J, He S, Li Q, Shoemaker BA, Thiessen PA, Yu B, Zaslavsky L. PubChem 2019 update: improved access to chemical data. *Nucleic acids research*. 2019 Jan 8;47(D1):D1102-9.

- [16] Yuan S, Chan HS, Hu Z. Using PyMOL as a platform for computational drug design. Wiley Interdisciplinary Reviews: Computational Molecular Science. 2017 Mar;7(2):e1298.
- [17] Bao, Y., Wang, W., Zhou, Z., & Sun, C. (2014). Benefits and risks of the hormetic effects of dietary isothiocyanates on cancer prevention. PLoS One, 9(12), e114764.
- [18] Maina, S., Misinzo, G., Bakari, G., & Kim, H. Y. (2020). Human, animal and plant health benefits of glucosinolates and strategies for enhanced bioactivity: A systematic review. Molecules, 25(16), 3682.
- [19] Deng, Q., Zinoviadou, K. G., Galanakis, C. M., Orlie, V., Grimi, N., Vorobiev, E., ...&Barba, F. J. (2015). The effects of conventional and non-conventional processing on glucosinolates and its derived forms, isothiocyanates: extraction, degradation, and applications. Food Engineering Reviews, 7(3), 357-381.
- [20] Al-Gendy, A. A., Nematallah, K. A., Zaghoul, S. S., &Ayoub, N. A. (2016). Glucosinolates profile, volatile constituents, antimicrobial, and cytotoxic activities of Lobularialibya. Pharmaceutical biology, 54(12), 3257-3263.
- [21] Jaafar, N. S., &Jaafar, I. S. (2019). Eruca sativa Linn.:Pharmacognostical and pharmacological properties and pharmaceutical preparations. Asian J Pharm Clin Res, 12(3), 39-45.
- [22] Bao, Y., Wang, W., Zhou, Z., & Sun, C. (2014). Benefits and risks of the hormetic effects of dietary isothiocyanates on cancer prevention. PLoS One, 9(12), e114764.
- [23] Choi, K. D., Kim, H. Y., & Shin, I. S. (2017). Antifungal activity of isothiocyanates extracted from horseradish (*Armoracia rusticana*) root against pathogenic dermal fungi. Food science and biotechnology, 26(3), 847-852.
- [24] Chaudhary, A., Sharma, U., Vig, A. P., Singh, B., &Arora, S. (2014). Free radical scavenging, antiproliferative activities and profiling of variations in the level of phytochemicals in different parts of broccoli (*Brassica oleracea italica*). Food chemistry, 148, 373-380.
- [25] Liu, P., Behray, M., Wang, Q., Wang, W., Zhou, Z., Chao, Y., &Bao, Y. (2018). Anti-cancer activities of allylisothiocyanate and its conjugated silicon quantum dots. Scientific reports, 8(1), 1-11.
- [26] Chaudhary, A., Sharma, U., Vig, A. P., Singh, B., &Arora, S. (2014). Free radical scavenging, antiproliferative activities and profiling of variations in the level of phytochemicals in different parts of broccoli (*Brassica oleracea italica*). Food chemistry, 148, 373-380.
- [27] Pocasap, P., Weerapreeyakul, N., &Thumanu, K. (2019). Alyssin and iberin in cruciferous vegetables exert anticancer activity in HepG2 by increasing intracellular reactive oxygen species and tubulin depolymerization. Biomolecules & therapeutics, 27(6), 540.
- [28] Fujioka, N., Fritz, V., Upadhyaya, P., Kassie, F., & Hecht, S. S. (2016). Research on cruciferous vegetables, indole-3-carbinol, and cancer prevention: A tribute to Lee W. Wattenberg. Molecular nutrition & food research, 60(6), 1228-1238.

- [29] Ryder, T. F., Calabrese, M. F., Walker, G. S., Cameron, K. O., Reyes, A. R., Borzilleri, K. A., & Kalgutkar, A. S. (2018). Acyl glucuronide metabolites of 6-chloro-5-[4-(1-hydroxycyclobutyl) phenyl]-1 H-indole-3-carboxylic acid (PF-06409577) and related indole-3-carboxylic acid derivatives are direct activators of adenosine monophosphate-activated protein kinase (AMPK). *Journal of medicinal chemistry*, 61(16), 7273-7288; Melong, R., Dzoyem, J. P., Tsamo, A. T., Kapche, D. G., Ngadjui, B. T., McGaw, L. J., & Eloff, J. N. (2018). Inhibitory effects of four naturally occurring compounds from *Epicoccumnigrum* on acetylcholinesterase activity and nitric oxide production in LPS-activated RAW 264.7 cells. *Investig Med ChemiPharmacol*, 1, 18.
- [30] Chitra, G., Franklin, D. S., Sudarsan, S., Sakthivel, M., & Guhanathan, S. (2017). Indole-3-acetic acid/diol based pH-sensitive biological macromolecule for antibacterial, antifungal and antioxidant applications. *International journal of biological macromolecules*, 95, 363-375.
- [31] Gong, G., Guan, Y. Y., Zhang, Z. L., Rahman, K., Wang, S. J., Zhou, S., ... & Zhang, H. (2020). Isorhamnetin: a review of pharmacological effects. *Biomedicine & Pharmacotherapy*, 128, 110301.
- [32] Ursu O, Rayan A, Goldblum A, Oprea TI. Understanding drug-likeness. *Wiley Interdisciplinary Reviews: Computational Molecular Science*. 2011 Sep;1(5):760-81.
- [33] Binkowski TA, Naghibzadeh S, and Liang J. CASTp: computed atlas of surface topography of proteins. *Nucleic acids research*. 2003 Jul 1; 31(13):3352-5.
- [34] NS, Syed K, Tuszynski J. Software for molecular docking: a review. *Biophysical reviews*. 2017 Apr 1;9(2):91-102.
- [35] Rizvi, S. M. D., Shakil, S., & Haneef, M. (2013). A simple click by click protocol to perform docking: AutoDock 4.2 made easy for non-bioinformaticians. *EXCLI journal*, 12, 831.
- [36] Afriza, D., Suriyah, W. H., & Ichwan, S. J. A. (2018, August). In silico analysis of molecular interactions between the anti-apoptotic protein survivin and dentatin, nordentatin, and quercetin. In *Journal of Physics: Conference Series* (Vol. 1073, No. 3, p. 032001). IOP Publishing.
- [37] Jejurikar, B. L., & Rohane, S. H. (2021). Drug Designing in Discovery Studio. *Asian Journal of Research in Chemistry*, 14(2), 135-138.
- [38] Ancona-Lezama, D., Dalvin, L. A., & Shields, C. L. (2020). Modern treatment of retinoblastoma: A 2020 review. *Indian journal of ophthalmology*, 68(11), 2356.
- [39] Beniwal, V., Maheshwari, G., Beniwal, S., Dhanawat, A., Tantia, P., & Adlakha, P. (2022). Retinoblastoma: A review of clinical profile at a regional cancer center in Northwest India. *Laterality*, 3(10), 18-5.
- [40] Fassl, A., Geng, Y., & Sicinski, P. (2022). CDK4 and CDK6 kinases: From basic science to cancer therapy. *Science*, 375(6577), eabc1495.
- [41] Tian, W., Chen, C., Lei, X., Zhao, J., & Liang, J. (2018). CASTp 3.0: computed atlas of surface topography of proteins. *Nucleic acids research*, 46(W1), W363-W367.

- [42] Matboli, M., Saad, M., Hasanin, A. H., Saleh, L. A., Baher, W., Bekhet, M. M., & Eissa, S. (2021). New insight into the role of isorhamnetin as a regulator of insulin signaling pathway in type 2 diabetes mellitus rat model: Molecular and computational approach. *Biomedicine & Pharmacotherapy*, 135, 111176.
- [43] Jia, M., Wei, Z., Liu, P., & Zhao, X. (2016). Silencing of ABCG2 by microRNA-3163 inhibits multidrug resistance in retinoblastoma cancer stem cells. *Journal of Korean medical science*, 31(6), 836-842.